

# First Measurement of the Neutron $\beta$ -Asymmetry with Ultracold Neutrons

R. W. Pattie Jr.,<sup>1,2</sup> J. Anaya,<sup>3</sup> H. O. Back,<sup>1,2</sup> J. G. Boissevain,<sup>3</sup> T. J. Bowles,<sup>3</sup> L. J. Broussard,<sup>2,4</sup> R. Carr,<sup>5</sup> D. J. Clark,<sup>3</sup> S. Currie,<sup>3</sup> S. Du,<sup>1</sup> B. W. Filippone,<sup>5</sup> P. Geltenbort,<sup>6</sup> A. García,<sup>7</sup> A. Hawari,<sup>1</sup> K. P. Hickerson,<sup>5</sup> R. Hill,<sup>3</sup> M. Hino,<sup>8</sup> S. A. Hoedl,<sup>7,9</sup> G. E. Hogan,<sup>3</sup> A. T. Holley,<sup>1</sup> T. M. Ito,<sup>3,5</sup> T. Kawai,<sup>8</sup> K. Kirch,<sup>3</sup> S. Kitagaki,<sup>10</sup> S. K. Lamoreaux,<sup>3</sup> C.-Y. Liu,<sup>9</sup> J. Liu,<sup>5</sup> M. Makela,<sup>3,11</sup> R. R. Mammei,<sup>11</sup> J. W. Martin,<sup>5,12</sup> D. Melconian,<sup>7,13</sup> N. Meier,<sup>1</sup> M. P. Mendenhall,<sup>5</sup> C. L. Morris,<sup>3</sup> R. Mortensen,<sup>3</sup> A. Pichlmaier,<sup>3</sup> M. L. Pitt,<sup>11</sup> B. Plaster,<sup>5,14</sup> J. C. Ramsey,<sup>3</sup> R. Rios,<sup>3,15</sup> K. Sabourov,<sup>1</sup> A. Sallaska,<sup>7</sup> A. Saunders,<sup>3</sup> R. Schmid,<sup>5</sup> S. Seestrom,<sup>3</sup> C. Servicky,<sup>1</sup> S. K. L. Sjue,<sup>7</sup> D. Smith,<sup>1</sup> W. E. Sondheim,<sup>3</sup> E. Tatar,<sup>15</sup> W. Teasdale,<sup>3</sup> C. Terai,<sup>1</sup> B. Tipton,<sup>5</sup> M. Utsuro,<sup>8</sup> R. B. Vogelaar,<sup>11</sup> B. W. Wehring,<sup>1</sup> Y. P. Xu,<sup>1</sup> A. R. Young,<sup>1,2</sup> and J. Yuan<sup>5</sup>

(The UCNA Collaboration)

<sup>1</sup>*Department of Physics, North Carolina State University, Raleigh, North Carolina 27695, USA*

<sup>2</sup>*Triangle Universities Nuclear Laboratory, Durham, North Carolina 27708, USA*

<sup>3</sup>*Los Alamos National Laboratory, Los Alamos, New Mexico 87545, USA*

<sup>4</sup>*Department of Physics, Duke University, Durham, North Carolina 27708, USA*

<sup>5</sup>*Kellogg Radiation Laboratory, California Institute of Technology, Pasadena, California 91125, USA*

<sup>6</sup>*Institut Laue-Langevin, 38042 Grenoble Cedex 9, France*

<sup>7</sup>*Physics Department, University of Washington, Seattle, Washington 98195, USA*

<sup>8</sup>*Research Reactor Institute, Kyoto University, Kumatori, Osaka, 590-0401, Japan*

<sup>9</sup>*Physics Department, Princeton University, Princeton, New Jersey 08544, USA*

<sup>10</sup>*Tohoku University, Sendai 980-8578, Japan*

<sup>11</sup>*Department of Physics, Virginia Tech, Blacksburg, Virginia 24061, USA*

<sup>12</sup>*Department of Physics, University of Winnipeg, Winnipeg, MB R3B 2E9, Canada*

<sup>13</sup>*Cyclotron Institute, Texas A&M University, College Station, Texas 77843, USA*

<sup>14</sup>*Department of Physics and Astronomy, University of Kentucky, Lexington, Kentucky 40506, USA*

<sup>15</sup>*Department of Physics, Idaho State University, Pocatello, Idaho 83209, USA*

(Dated: October 23, 2018)

We report the first measurement of angular correlation parameters in neutron  $\beta$ -decay using polarized ultracold neutrons (UCN). We utilize UCN with energies below about 200 neV, which we guide and store for  $\sim 30$  s in a Cu decay volume. The  $\vec{\mu}_n \cdot \vec{B}$  potential of a static 7 T field external to the decay volume provides a 420 neV potential energy barrier to the spin state parallel to the field, polarizing the UCN before they pass through an adiabatic fast passage (AFP) spin-flipper and enter a decay volume, situated within a 1 T,  $2 \times 2\pi$  superconducting solenoidal spectrometer. We determine a value for the  $\beta$ -asymmetry parameter  $A_0$ , proportional to the angular correlation between the neutron polarization and the electron momentum, of  $A_0 = -0.1138 \pm 0.0051$ .

PACS numbers: 12.15Ff, 12.15Hh, 13.30Ce, 23.40Bw

Measurements of neutron  $\beta$ -decay observables provide fundamental information on the parameters characterizing the weak interaction of the nucleon. Results from such measurements can be used to extract a value for the CKM quark-mixing matrix element  $V_{ud}$  and impact predictions for the solar neutrino flux, big bang nucleosynthesis, the spin content of the nucleon, and tests of the Goldberger-Treiman relation [1]. High-precision results also place constraints on various extensions to the standard model, such as supersymmetry [2] and left-right symmetries [3]. Angular correlation measurements in neutron  $\beta$ -decay have been performed with thermal and cold neutron beams [4], including all previously reported measurements of the  $\beta$ -asymmetry [5, 6, 7, 8, 9]. The use of UCN for these measurements provides a different and powerful approach to controlling key sources of systematic errors in measurements of polarized neutron  $\beta$ -decay: the preparation of highly polarized neutrons and the backgrounds intrinsic to the neutron  $\beta$ -decay sample.

The  $\beta$ -asymmetry results from the angular correlation between the neutron spin and the electron momentum, where the angular distribution of emitted electrons is

$$W(E_e, \theta) = F(E_e)(1 + A\langle P\rangle\beta \cos\theta). \quad (1)$$

Here,  $E_e$  and  $\beta$  are the electron energy and velocity relative to  $c$ ,  $F(E_e)$  is the allowed shape of the electron energy spectrum,  $\langle P\rangle$  is the neutron polarization, and  $\theta$  is the angle between the neutron spin and the electron momentum. The magnitude of the asymmetry is the  $A$  parameter [10, 11, 12], given by  $A = A_0(1 + a_0 + a_{-1}/E_e + a_{+1}E_e)(1 + \delta)$ , where  $A_0 = -2\lambda(\lambda + 1)/(1 + 3\lambda^2)$ . The recoil order terms  $a_0$ ,  $a_{-1}$ ,  $a_{+1}$  and the radiative correction  $\delta$  are specified in the standard model in terms of six effective coupling constants, with leading-order contributions from two form factors ( $g_v$  and  $g_a$ , the vector and axial-vector coupling constants with  $\lambda \equiv g_a/g_v$ ) and one form factor which only appears in the recoil order terms ( $g_{wm}$ , the weak magnetism coupling constant). The other three

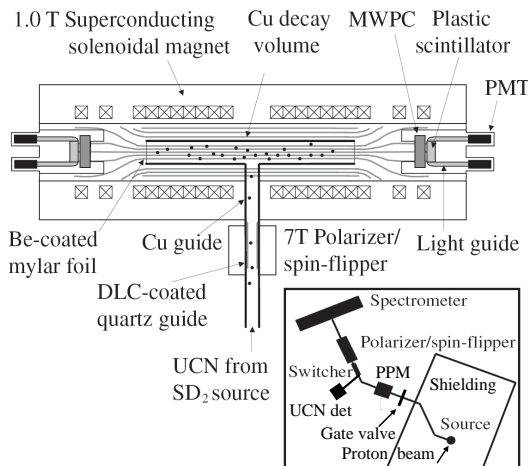


FIG. 1: Schematic (not to scale) of the  $\beta$ -asymmetry experiment. Inset depicts the layout of the UCN source and transport guides.

form factors are expected to be negligible at the level of precision of this work. Very precise estimates for  $g_v$  and  $g_{wm}$  are available in the standard model, but precise theoretical predictions for  $g_a$  are not available. Other than  $g_a$ , limiting theoretical uncertainties are below the 0.1% level, and stem from hadronic loop contributions to radiative corrections [13].

UCN are defined as neutrons with energies low enough ( $\lesssim 340$  neV) that they undergo total external reflection from an effective potential barrier  $E_{\text{Fermi}}$  at some material surfaces [14] and can therefore be stored in material bottles. We produced UCN in a solid deuterium ( $\text{SD}_2$ ) source [15] closely coupled to a tungsten spallation target in the 800 MeV proton beam at the Los Alamos Neutron Science Center (LANSCE). Protons were delivered in 28  $\mu\text{C}$  pulses, once every 17 s, with the spallation neutrons moderated in cold ( $\sim 20$  K) polyethylene surrounding the source. UCN were created via downscattering of the resulting cold neutron flux in 5 K  $\text{SD}_2$ . After each proton pulse, the emerging UCN passed through a valve located above the  $\text{SD}_2$ . This valve was then immediately closed, loading a storage volume (20 l vertical volume and 40 l of guides) above the  $\text{SD}_2$  with UCN, at an estimated density of  $10 \text{ UCN cm}^{-3}$  at the exit of the spallation source shielding. The vertical storage volume was coupled by about 5 m of electropolished stainless steel guides (with two  $45^\circ$  bends to limit backgrounds) to a gate valve just beyond the shielding, and then ultimately to a switcher which allowed the guides comprising the  $\beta$ -asymmetry experiment (schematic shown in Fig. 1) to be connected either to the UCN source or a  $^3\text{He}$  UCN detector for depolarization measurements, described below.

One of the primary advantages of the low UCN energy is the ability to highly polarize a UCN population using the  $\vec{\mu}_n \cdot \vec{B}$  potential associated with a static magnetic field, which amounts to  $\pm 60 \text{ neV T}^{-1}$  for neutron spins

aligned(+)/anti-aligned(-) with the field. The UCN flux was polarized via this effect, using a longitudinal 6 T field in a pre-polarizer magnet (PPM) and a 7 T field in the primary polarizer/spin-flipper magnet. The polarization of the subsequent population was maintained by polarization-preserving electropolished Cu ( $E_{\text{Fermi}} \approx 168$  neV) guides and a 100-cm long diamond-like carbon (DLC) coated quartz section ( $E_{\text{Fermi}} > 200$  neV) passing through the center of a resonant “birdcage” rf cavity used for adiabatic fast passage (AFP) spin flipping of the UCN. Holding fields were established by the homogeneous 1 T field in the spectrometer, and the superposition of the magnets’ fringe fields in the connecting region.

Prior to the  $\beta$ -asymmetry run, a measurement of the AFP spin-flipper efficiency was made by placing the PPM magnet in the section which normally connects the polarizer/spin-flipper magnet with the spectrometer, creating a crossed polarizer analyzer with the PPM utilized as the analyzer. In order to increase the analyzing power of the PPM (whose maximum field was limited to 6 T), a  $\sim 13 \mu\text{m}$  thick Cu-coated kapton foil was placed in the high-field region. The transmission through the system was measured to be 0.40(5)%, placing a lower limit of 99.1% on the initial UCN polarization and a lower limit of 99.6% on the spin-flipper efficiency. Based on spectral measurements and limitations of the PPM/foil analyzer we expect the actual values of the initial UCN polarization and spin-flipper efficiency to be higher; however, the lower limits presented here were used in our estimates of polarization-related systematics.

In order to measure the depolarization on a run-by-run basis, the measurement cycle consisted of a background run (with proton beam on, but gate valve closed, resulting in no UCN in the spectrometer,  $\sim 720$  s in duration) followed by the  $\beta$ -asymmetry measurement for some spin-state ( $\sim 3600$  s), and then a measurement of the depolarized population ( $\sim 240$  s). The depolarization measurement consisted of first closing the gate valve while simultaneously connecting the guides at the upstream side of the experiment to the  $^3\text{He}$  UCN detector using the switcher. This cleaning phase, lasting 150 s, allowed the number of correctly polarized UCN downstream of the 7 T polarizing field to be measured. Next, the depolarized population present in the experiment was unloaded and counted by changing the state of the spin-flipper. Counting during this unloading cycle was carried out for 100 s after which the next measurement cycle was started. The depolarized contamination at the end of each individual run was consistent with zero. By combining all available runs, correcting for depolarized UCN detection efficiency, and attributing the crossed polarized analyzer result entirely to unpolarized UCN, we were able to place an upper limit ( $1\sigma$ ) of 0.65% on the depolarized fraction present during any individual run. We expect that better characterization of our

system combined with significant improvements in background and statistics during depolarized UCN counting should result in a limit below 0.2% in the future.

After transport to the spectrometer, the UCN were confined to a 300-cm long, 12-cm diameter Cu decay trap tube with end-cap foils consisting of 2.5- $\mu\text{m}$  thick mylar foils coated with 300 nm of Be. Storage times of  $\sim 30$  s were achieved. A plastic collimator with an inner diameter of 11.7 cm, which also functioned as the end-cap foil mount, suppressed contamination from electrons scattering from the Cu decay trap or resulting from neutron capture on the Cu walls. The spectrometer’s 1 T solenoidal field was oriented along the decay trap axis and provided for  $2 \times 2\pi$  collection of the  $\beta$ -decay electrons, which spiraled along the field lines toward one of two identical electron detector packages [16]. This expansion of the field from 1 T in the decay region to 0.6 T in the detector region suppresses electron backscattering (scattering at angles  $> 90^\circ$  relative to incidence) via two mechanisms. First, pitch angles of  $90^\circ$  in the 1 T region map to  $51^\circ$  in the 0.6 T region. Second, electrons which backscatter at pitch angles  $\theta > 51^\circ$  are reflected via the magnetic mirror effect back into the same detector.

The two electron detector packages [17, 18] each consisted of a low-pressure (132 mbar) multiwire proportional chamber (MWPC) backed by a 3.5 mm thick, 15 cm diameter plastic scintillator, and were spaced 4.4 m apart. Requiring a coincidence between the same-side MWPC and scintillator led to a significant reduction in backgrounds. The MWPCs also permitted reconstruction (with 2 mm resolution) of the events’ transverse coordinates, for the rejection of events originating near the edge of the collimator. The position sensitivity of our MWPCs ensured “edge effects” associated with electron scatter from the walls of our decay trap or collimator edges were negligible. The MWPCs were separated from the spectrometer vacuum and the scintillator volumes by identical 25  $\mu\text{m}$  thick mylar entrance and exit windows.

The scintillator generated the trigger and provided for the energy measurement. Energy calibrations were performed *in situ* every 6–8 hours, using a  $^{113}\text{Sn}$  source of conversion electrons which could be inserted and retracted from the spectrometer’s fiducial volume. Gain variations between calibrations were monitored and corrected for by comparing the response of the scintillator and an external photomultiplier tube (PMT) to a pulsed LED source. The response of the external PMT to the LED was normalized to the spectrum of gamma rays from a  $^{60}\text{Co}$  source in a NaI crystal coupled to this PMT.

The linearity of the detector response was studied at the conclusion of the run with a limited selection of conversion-electron sources ( $^{113}\text{Sn}$  and  $^{207}\text{Bi}$ ), effectively calibrating the detectors. Analysis of the implementation of our calibration via Monte Carlo suggests a (conservative) 1.5% uncertainty in the value for  $A_0$  due to possible errors in our electron energy reconstruction. Note that

TABLE I: Fractional systematic corrections to  $A_0$ .

Systematic	Correction	Uncertainty
Polarization	—	0.013
UCN-Induced Backgrounds	—	0.002
Electron Detector Effects		
Response/Linearity	—	0.015
Width/Pedestal	—	0.001
Gain Drifts	—	0.002
Electron Trajectories		
Angle Effects	−0.016	0.005
Backscattering	0.011	0.004
Total	$-5 \times 10^{-3}$	0.021

with these calibration studies, the resolution of the scintillator was shown to be 5.6% at 1 MeV.

The spectrometer was surrounded by a cosmic-ray muon veto system consisting of proportional gas tubes and plastic scintillator. Proton beam-related backgrounds were suppressed with timing cuts. A significant potential advantage of UCN over cold neutron beams for angular correlation measurements stems from the relatively small number of neutrons present in the decay geometry and guides. Because the absolute efficiency of an MWPC-scintillator coincidence detection of neutron-generated gamma-ray backgrounds within the fiducial volume is extremely small compared to the nearly 100% electron-detection efficiency, UCN-generated backgrounds were negligible.

Misidentification of backscattering events is one of the largest contributions to the total fractional systematic correction to the value for  $A_0$  reported here (see Table I). Electrons triggering both scintillators within a 100 ns acceptance window comprised 2.5(3)% of all events, with the initial direction of incidence determined by the scintillators’ relative trigger times. The bias to the asymmetry from events with transit times greater than 100 ns is small,  $< 10^{-5}$ . Another class of backscattering events, comprising 1.4(2)% of the event fraction, were those events which triggered only one of the scintillators, but deposited energy in both MWPCs. Comparison of the energy deposition in the MWPCs determines the initial direction of incidence for these events, with the efficiency for this identification calculated in Monte Carlo to be  $\sim 80\%$ . Finally, events which backscattered from either the decay trap end-cap foils or the MWPC entrance windows could not be identified in data analysis, and are termed “missed” backscattering events. Corrections for these missed backscattering events were separately performed using the GEANT4 [19] and PENELOPE [20] simulation packages, and found to be 1.1(4)%. Previous studies of these Monte Carlo backscattering calculations suggest a (conservative) 30% uncertainty in the missed backscattering correction [21].

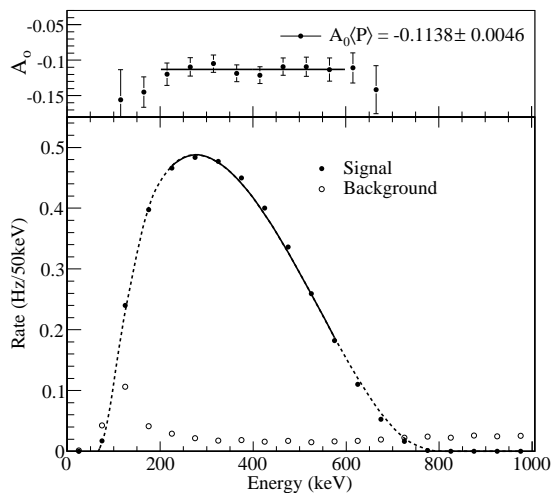


FIG. 2: Top panel: Values for  $A_0$  extracted from the best fit, varying the parameter  $\lambda$ , plotted as a function of the reconstructed  $\beta$ -decay energy (i.e., after accounting for energy loss; see text for details). The value of  $\delta$  is below 0.1% [22] and therefore negligible for this study. Bottom panel: Reconstructed  $\beta$ -decay energy spectrum, summed over detectors, compared with the expectation from Monte Carlo (dashed line). Solid line indicates analysis region.

Linear parametrizations of energy loss in the decay trap end-cap foils and the MWPC entrance/exit windows and interior were employed to reconstruct, on an event-by-event basis for each event type, the  $\beta$ -decay energy from the measured energy deposition in the scintillator(s). The resulting energy spectrum, compared to background, is shown in Fig. 2. Disagreement between the shape of the reconstructed energy spectrum and that expected from simulation is  $< 3\%$  over the chosen analysis region of 200–600 keV. The lower limit of 200 keV was constrained by energy loss for backscattering events triggering both scintillators. The upper limit of 600 keV was an optimization of the signal-to-noise ratio, seen in Fig. 2 to be 21:1 from 200–600 keV, over 0.17 Hz of background. Note that the background-subtracted rate above the  $\beta$ -decay endpoint was consistent with zero.

Due to the angle dependence of the energy loss, the average value of  $\cos\theta$  deviates from 1/2 and varies as a function of energy. The correction to the asymmetry for such “angle effects” was calculated in Monte Carlo to be  $-1.6(5)\%$ . Effects due to differences in loading efficiencies for the two spin states and detector efficiencies cancel in a super ratio of rates,  $S(E_e) = r(E_e)_1^\uparrow r(E_e)_2^\downarrow / r(E_e)_1^\downarrow r(E_e)_2^\uparrow$ , where  $r(E_e)_i^{\uparrow(\downarrow)}$  was the rate measured in detector 1(2) when the spin-flipper was on(off). The experimental asymmetry is then  $A(E_e) = (1 - \sqrt{S(E_e)}) / (1 + \sqrt{S(E_e)})$ . After correcting for backscattering and angle effects,  $A_0$  was extracted from a one-parameter fit. With these corrections we find  $A_0 = -0.1138(46)(21)$ , where the first (second) uncertainty is statistical (systematic). Results for  $A_0$  from in-

dependent analyses utilizing PENELOPE or GEANT4 for calculation of the corrections for energy loss and backscattering agreed to 0.26%.

In summary, we have demonstrated the first-ever measurement of a neutron  $\beta$ -decay angular correlation parameter with UCN. Subsequent improvements in the UCN transport to the spectrometer will lead to a reduction in the statistical error. Significant improvements in the limits placed on the fraction of depolarized UCN should follow from improved statistics for depolarization studies and improved operating parameters for our  $^3\text{He}$  UCN detectors. A transition to thinner decay trap end-cap foils and MWPC windows will reduce the magnitude of the systematic corrections for backscattering and angle effects, and a greater selection of calibration sources will be employed for more extensive studies of the detector response.

This work was supported in part by the Department of Energy, National Science Foundation, and Los Alamos National Laboratory LDRD. We acknowledge helpful discussions with A. P. Serebrov.

- 
- [1] A. Czarnecki, W. J. Marciano, and A. Sirlin, *Phys. Rev. D*, **70**, 093006 (2004).
  - [2] K. Hagiwara, S. Matsumoto, and Y. Yamada, *Phys. Rev. Lett.* **75**, 3605 (1995); A. Kurylov and M. J. Ramsey-Musolf, *Phys. Rev. Lett.* **88**, 071804 (2002).
  - [3] N. Severijns, M. Beck, and O. Naviliat-Cuncic, *Rev. Mod. Phys.* **78**, 991 (2006).
  - [4] J. S. Nico and W. M. Snow, *Ann. Rev. Nucl. Part. Sci.* **55**, 27 (2005).
  - [5] H. Abele *et al.*, *Phys. Rev. Lett.* **88**, 211801 (2002); J. Reich *et al.*, *Nucl. Instrum. Methods Phys. Res. A* **440**, 535 (2000); H. Abele *et al.*, *Phys. Lett. B* **407**, 212 (1997).
  - [6] P. Liaud *et al.*, *Nucl. Phys. A* **612**, 53 (1997).
  - [7] B. G. Erokolimskii *et al.*, *Phys. Lett. B* **263**, 33 (1991); B. G. Erokolimskii *et al.*, *Sov. J. Nucl. Phys.* **52**, 999 (1990); B. G. Yerozolimsky *et al.*, *Phys. Lett. B* **412**, 240 (1997), Yu. A. Mostovoi *et al.*, *Phys. Atom. Nucl.* **64**, 1955 (2001).
  - [8] P. Bopp *et al.*, *Phys. Rev. Lett.* **56**, 919 (1986); *Nucl. Instrum. Methods Phys. Res. A* **267**, 436 (1988).
  - [9] V. E. Krohn and G. R. Ringo, *Phys. Lett.* **55B**, 175 (1975); C. J. Christensen *et al.*, *Phys. Lett.* **28B**, 411 (1969).
  - [10] B. R. Holstein, *Rev. Mod. Phys.* **46**, 789 (1974).
  - [11] S. Gardner and C. Zhang, *Phys. Rev. Lett.* **86**, 5666 (2001).
  - [12] J. D. Jackson, S. B. Trieman, and H. W. Wyld, Jr., *Phys. Rev.* **106**, 517 (1957).
  - [13] W. J. Marciano and A. Sirlin, *Phys. Rev. Lett.* **96**, 032002 (2006).
  - [14] R. Golub, D. J. Richardson, and S. K. Lamoreaux, *Ultra-Cold Neutrons* (Adam Hilger: Bristol, 1991).
  - [15] A. Saunders *et al.*, *Phys. Lett. B* **593**, 55 (2004); C. L. Morris *et al.*, *Phys. Rev. Lett.* **89**, 272501 (2002).
  - [16] In the current geometry, UCN are confined to the decay

- trap, located in a uniform field region, ensuring magnetic mirroring corrections to  $A_0$  due to UCN decays in non-uniform fields are below the 0.1% level.
- [17] T. M. Ito *et al.*, Nucl. Instrum. Methods Phys. Res. A **571**, 676 (2007).
  - [18] B. Plaster *et al.*, arXiv:0806.2097, to appear in Nucl. Instrum. Methods Phys. Res. A.
  - [19] S. Agostinelli *et al.*, Nucl. Instrum. Methods Phys. Res. A **506**, 250 (2003); <http://geant4.cern.ch/> .
  - [20] F. Salvat, J. M. Fernández-Varea, and J. Sempau, *PENELOPE – A Code System for Monte Carlo Simulation of Electron and Photon Transport*, Universitat de Barcelona, Spain (2003).
  - [21] J. W. Martin *et al.*, Phys. Rev. C **68**, 055503 (2003); J. W. Martin *et al.*, Phys. Rev. C **73**, 015501 (2006).
  - [22] F. Gluck and K. Toth, Phys. Rev. D **46** 2090 (1992).